Article

Evaluation of a UAV-Assisted Autonomous Water Sampling

Cengiz Koparan [1], Ali Bulent Koc [1,*], Charles V. Privette [1], Calvin B. Sawyer [1]
and Julia L. Sharp [2]

[1] Department of Agricultural Sciences, Clemson University, Clemson, SC 29634-0310, USA;
    ckopara@g.clemson.edu (C.K.); privett@clemson.edu (C.V.P.); calvins@clemson.edu (C.B.S.)
[2] Department of Statistics, Colorado State University, Fort Collins, CO 80523-1877, USA; jlsharp@colostate.edu
*   Correspondence: bulent@clemson.edu; Tel.: +1-864-656-0496

check for
updates

Abstract: Water quality assessment programs for the management of water resources require the collection of water samples for physical, chemical, and biological analyses. Lack of personnel, accessibility of water bodies, and time constraints, especially after natural disasters and emergencies, are some of the challenges of water sampling. To overcome these challenges, a custom-made thief-style water sampling mechanism was developed and mounted on a multirotor unmanned aerial vehicle (UAV) for autonomous water sampling. The payload capacity and endurance of the UAV were determined using an indoor test station. The UAV was equipped with floatation, and electronic components were coated to prevent water damage in the event of a forced landing or for sample collection. Water samples from a 1.1 ha pond were collected with the developed UAV-assisted water sampling system and traditional manual methods. Dissolved oxygen (DO), electrical conductivity (EC), pH, temperature and chloride measurements were made on samples collected with both UAV-assisted and manual methods and compared. Percent differences between the two sampling methods for DO, EC, pH, and temperature were minimal except for chloride level. Percent differences between the two sampling methods for DO, EC, pH, and temperature measurements were 3.6%, 2.3%, 0.76%, and 0.03%, respectively. Measured chloride levels for the manual and UAV-assisted sampling methods were 3.97 and 5.46 mg/L. UAV-assisted water sampling may prove faster and safer than manual water sampling from large surface waters and from difficult to access water bodies.

Keywords: water quality; sampling; UAV; dissolved oxygen; electrical conductivity; temperature

1. Introduction

Water quality monitoring is necessary for effective management of water resources. Periodic sampling and analysis allows one to characterize water and identify changes or trends in water quality over time. For example, pollutants carried by stormwater may include bacteria, nutrients, litter, sediment, oils, and heavy metals [1]. Through monitoring, information can be gathered to implement specific pollution prevention and remediation programs. Water quality monitoring can provide a check on whether pollution prevention program goals are in compliance with regulations.

Streams receive pollutants from point and nonpoint sources [2]. Drainage channels, outlets from industrial plants, and wastewater treatment facilities are some of the point sources of inflow. Water pollutant entry from nonpoint sources occurs only after rainfall or emergency overflows during a short period. Nonpoint sources including impervious surfaces such as roadways, rooftops, parking lots, and sidewalks accumulate pollutants and convey them directly to lakes, rivers, and estuaries [3]. Runoff that heats up on parking lots and roadways can lead to warmer than normal water entering nearby

waterways that may cause increase in temperature of surface water. These sources can be monitored with event-controlled water samplers [4].

In addition to water sampling after a storm event, regular water sampling is also necessary to identify the entry points of pollutants into surface water. For example, nutrient leaching from farm fields or pasture lands to surface water could cause algal blooms. Growth of dense algal blooms causes discoloration in water bodies and can potentially result in damaging fluctuations of dissolved oxygen. Among algal blooms, blue-green algae has the genetic potential to produce toxins [5] that are harmful to humans and animals, and may cause death to livestock [6].

Current water quality monitoring in lakes and reservoirs may be done by volunteers with boats [7]. Volunteers make measurements at predefined locations and collect water samples for laboratory analyses. Water quality parameters measured include turbidity, temperature, algal chlorophyll, dissolved oxygen (DO), electrical conductivity (EC), pH, total phosphorous, nitrogen, and suspended solids. Temperature and pH are important indicators of water quality as they affect rates of biological and chemical activities. Water temperature varies according to the time of year, time of day, weather conditions, water depth, total dissolved solids, shading, and vegetation [8]. Aquatic organisms require certain pH ranges for survival. Monitoring pH levels in water can eliminate further damage to aquatic life and surrounding environment. The growth of aquatic organisms is greatly reduced if the pH is lower than 4 and greater than 10 in the water. A change in the pH can alter the behavior of other chemicals in the water which might make them toxic [9]. Because DO is a key indicator of biological activity [10], it is possible that the sampling mechanism might induce error in this parameter during sampling. Inland chloride ions naturally occur from dissolved minerals in most surface waters, and they come from lawn fertilizers and road salt [11]. Chloride ions are mobile in the soil and can be taken up by roots and accumulate in leaves resulting in toxicity. High concentration of chloride in organisms can induce osmotic stress and reduce fitness or mortality [12]. EC is an indicator of the presence of mineral salt and fertilizers, organic matter, and treated wastewater. EC measurements are used to identify existing problems in surface water for water quality monitoring.

Despite the availability of help from volunteers to monitor water quality, some lakes, retired mining zones, or other water bodies surrounded by steep and difficult terrain may not be accessible by boats. In addition, lakes with cyanobacteria (blue-green algae) blooms may cause risks to human while collecting water samples or making water quality measurements. Autonomous underwater vehicles (AUVs) and autonomous surface vehicles (ASVs) have been used for water quality monitoring in recent years [13,14]. The major challenge of water quality monitoring with an underwater vehicle is the accurate positioning of the vehicle as the GPS system cannot be used when the vehicle is underwater [14]. Because of this limitation, the AUVs have to be equipped with additional navigational systems or acoustic localization systems. The ASV can automatically navigate to predefined sampling points and measure pH, DO, EC, turbidity, temperature, sensor depth, water depth, chlorophyll-a concentration, and nitrates [13]. The disadvantages of automatic sampling with ASVs are the operational difficulties due to swaying from side to side and uncertain engine-control frequencies [13].

Unlike the above methods, unmanned aerial vehicles (UAVs) can also be used for water quality monitoring. UAVs are commonly used for remote sensing in agriculture for scouting of field crops and livestock monitoring [15]. Crop yield assessments, crop height monitoring, crop weed mapping, and biomass monitoring are some of the examples for remote sensing with a multispectral camera integrated UAVs [16–19]. UAVs can also acquire air quality data with high spatial and temporal resolution [20]. Recent developments in sensor technology led to the design of compact devices that can measure a variety of air pollutants [21]. The use of UAVs is not limited with remote sensing or air quality monitoring. UAVs are also used for aerial spraying of herbicides or pesticides, aerial sensing of sound and identifying changes in land structure for city planning [22,23]. Emergency applications of UAVs include but are not limited to blood delivery, ambulances for cardiac arrest, and disaster relief operations [24–26]. Distinct advantages that UAVs provide include the ability to rapidly and remotely travel to locations that are difficult to access and the efficient execution of tasks

with relatively reduced costs and time. For example, aerial images that are taken remotely with a UAV can help visualize disturbances in water and provide enhanced spatial water quality monitoring data [27,28]. Aerial surveys with a high-resolution camera attached to a UAV may also be used to monitor topographic changes in watersheds [29]. Information gathered from these surveys can provide the specific coordinates of contaminations, which can be included in water quality monitoring plan for further sampling. For example, a UAV-assisted in situ water quality measurement system was developed and tested over an agricultural pond [30]. The developed system can measure electrical conductivity, pH, dissolved oxygen, and the temperature of water autonomously [30]. In addition to water quality monitoring, a water sampling UAV with water collection devices can be used to collect water from pre-determined locations [31]. Ore et al. (2015) developed a multirotor UAV equipped with a water pump, sampling tube, and vial to collect three 20 mL samples per flight [31]. The use of a pump would require additional components and extend the time for water collection. A UAV with a rapid water-capturing mechanism can reduce the sample collection time.

The objective of this research was to evaluate the functions of a custom-made UAV-assisted autonomous water sampling system with laboratory and field tests.

2. Materials and Methods

2.1. Multirotor UAV

A custom-built multirotor UAV was used for this research. The manual control of the UAV was accomplished with a radio controller (RC) (Turnigy 9X, Hextronik, Chengdu, China). Autonomous control of the UAV was accomplished with a flight controller. The main components of the UAV were a frame, motors, propellers, electronic speed controllers, a flight controller (Pixhawk, 3DR, Robotics, Berkeley, CA, USA), a GPS receiver (Ublox, 3DR, Berkeley, CA, USA), a telemetry radio transmitter (3DR radio, 3DR, 3DR, Berkeley, CA, USA), and a power supply (Venom, Rathdrum, ID, USA). The total hull length of the UAV was 566 mm (Figure 1). The payload mounted at the bottom of the frame contained a servo motor, fabricated water capturing mechanism (FWCM), a messenger to trigger FWCM, and floatation attachments. Electronic parts were chosen depending on the desired payload, flight time, and compatibility [32]. The total payload capacity of a UAV depends on thrust it can produce. Therefore, water sampling capacity of the system was limited. Indoor experiments were conducted to determine flight duration of the UAV with water sampler. Specifications of UAV components used in this study are shown in Table 1.

Table 1. Specifications of unmanned aerial vehicle (UAV) components.

Part Name	Model/Number	Specifications	Function	Quantity	Weight (g)
Motors	T-Motor/MN3110	KV700	Main actuator	6	480 g
ESCs	Arris SimonK	30 A	Speed Control	6	150 g
Propellers	Andoer/1045	Carbon Fiber	Propelling	6	51 g
Microcontroller	Pixhawk	Open hardware	Flight Control	1	182 g
Battery (Li-Po)	Venom 14.8V	25C 4S 5000 mAh	Power Supply	1	542 g
Power Module	3DR-XT60	BEC 3A 5.3V 7S	Power distribution	1	28 g
RC receiver	9X 8Ch Mode2	2.4 GHz	Receive command	1	8.5 g
Radio receiver	3DR	433 MHz	Radio command	1	8.5 g
GPS	3DR-0003	Compass 5 Hz	GPS antenna	1	45 g
Servo	SG90	4.8 V (1 kg/cm)	Triggers sampler	1	9 g
Frame	F550	PCB wiring	Holds parts	1	678 g
Floating parts	N/A	753 cm^3	Provides floating	12	151 g
		TOTAL			2333 g

Note: ESCs, Electronic speed controllers.

A ground control station contained a computer which communicated with the UAV via a telemetry radio transmitter. The ground station gathered information about flight conditions including battery

level, altitude, location, flight mode situation, and GPS connection status during a flight mission. All electronic circuits in the system were waterproofed using a corrosion prevention spray (90102 Anti corrosion, Corrosion Technologies, Dallas, TX, USA) to prevent water damage to system components.
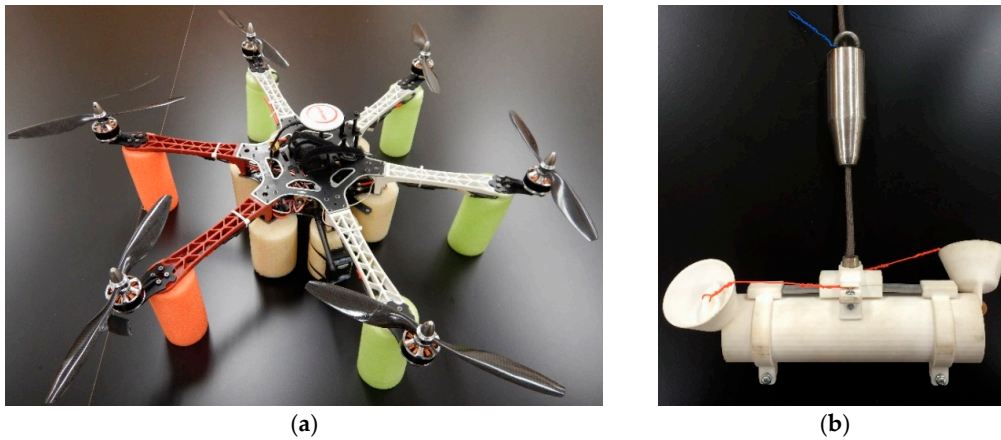

(**a**)   (**b**)

Figure 1. (**a**) The UAV with floating attachments; (**b**) fabricated water capturing mechanism (FWCM) and messenger.

2.2. Flight Performance Test Station

The endurance and total payload of the UAV were determined with indoor tests. A flight performance test station was developed to determine how long the UAV can fly while carrying a certain payload (Figure 2). The flight performance test station consisted of a wooden structure, a load cell (MR01, Honeywell, Morris Plains, NJ, USA), a data acquisition board (NI-USB-6009, National Instruments, Austin, TX, USA), and a bridge sensor (DMD 465, Omega Engineering, Norwalk, CT, USA). The test station was developed to place the UAV in the middle of the wooden columns to provide safe zone during the tests. The data acquisition board was used to transfer thrust measurements to a computer. Once the UAV was placed in the columns, it moved freely on the vertical axis. The load cell placed under the top cover of the station measured the force while the UAV was flying in the upward direction. Load cell was calibrated by converting real-time load values (g) into electrical signals (mV). The dynamic range of the load cell was 5–50 kg with an excitation voltage range of 5–10 V. The bridge sensor was integrated with the load cell for signal conditioning to amplify the full scale output voltage [33]. A regression equation was developed between the known weights and output voltages. The regression equation in the LabVIEW program then converted the output voltage into corresponding weight while the UAV was exerting force on the load cell in the upward direction.
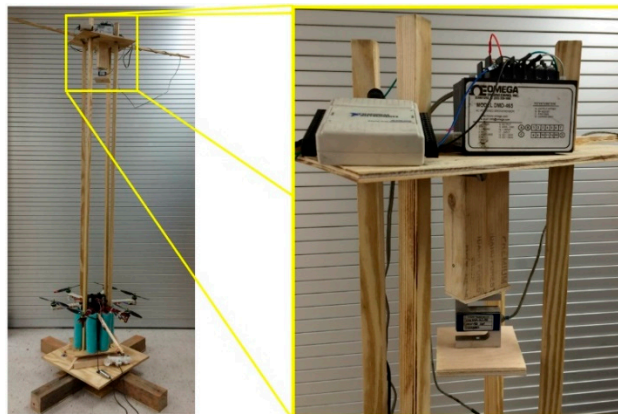

Figure 2. Indoor flight performance station.

The UAV was operated at different throttle (speed) settings. Varying the throttle level changed the speed of the motors and the amount of vertical force applied on the load cell in the upward direction. The force measurements taken from the load cell were used to determine the thrust that the UAV can produce at a given throttle level. From the thrust measurements, the payload (g) capacity of the UAV was determined. The gross weight of the UAV was determined from the payload and the empty weight of the UAV [34].

2.3. Fabricated Water Capturing Mechanism

A thief-style water sampler [35] was designed with SolidWorks® (Dassault Systèmes Americas Corp., Waltham, MA, USA) and fabricated. A thief sampler is typically an open tube used to sample containerized liquid water [36]. Designed parts were 3D-printed with a laser printer using Selective Laser Sintering (SLS) technique to fabricate the water capturing mechanism. The volumetric capacity of the sampling equipment was designed to be 130 mL. Figure 3 shows the FWCM. The FWCM consists of a cylindrical tube, tube covers, a release button, and a polymer plastic string. The length and diameter of the sampling tube were 15.24 and 3.81 cm, respectively. A polymer plastic tether was selected because of its strength and elasticity. This material provided enough tension to pull the covers back when the sampler was set. The plastic string closes the two open ends rapidly once the release button is pressed. The release button is pressed when the messenger (a metal weight) is released. Releasing the messenger and triggering the push button actions were achieved autonomously with the flight controller.
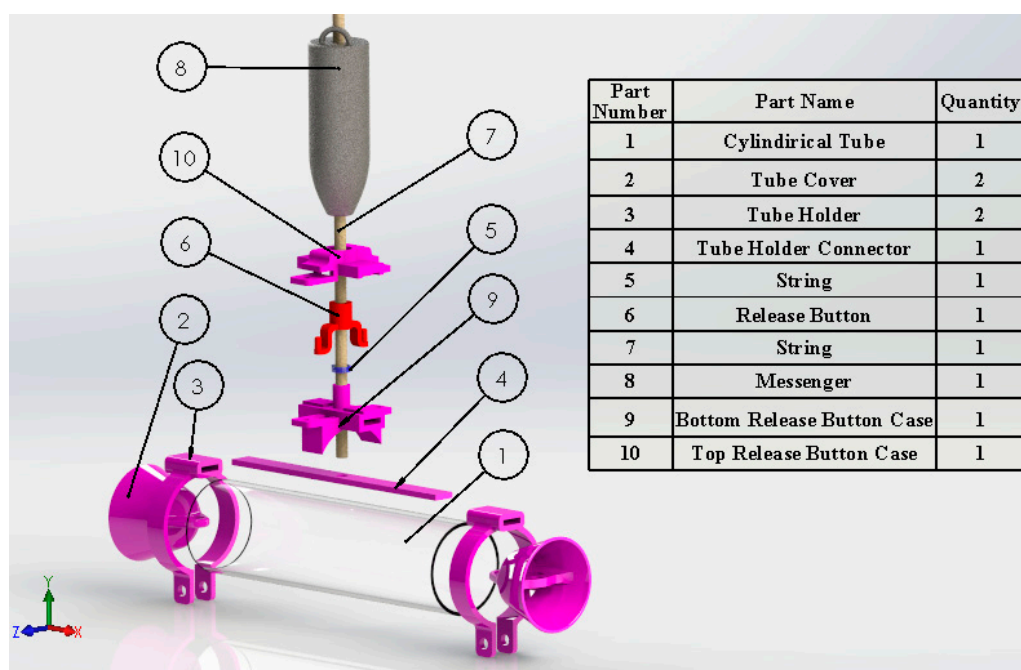

Part Number	Part Name	Quantity
1	Cylindirical Tube	1
2	Tube Cover	2
3	Tube Holder	2
4	Tube Holder Connector	1
5	String	1
6	Release Button	1
7	String	1
8	Messenger	1
9	Bottom Release Button Case	1
10	Top Release Button Case	1

Figure 3. Three-dimensional perspective view of the FWCM and its components.

A Pixhawk flight controller was used for the system. The Pixhawk flight controller is capable of acquiring data from various sensors and controlling different devices such as servo actuators [37]. Servos are commonly used as camera shutters or fixed winged model aircraft controls [38]. The Mission Planner ground control software enables servo control during an autonomous flight. With the help of the flight controller, the servo can be triggered at any pre-determined location at any desired altitude.

The developed UAV can fly autonomously using its autopilot function and automatically obtain altitude information from its sensors [39]. Therefore, the water sampler release action was controlled with autopilot commands. A "do-set-servo" command was added to the flight mission at a desired

location and altitude. Once the UAV is in hovering pattern over the sampling location, the servo is triggered to release the water sampler into the waterbody to collect a water sample. With the weight of the collected water, the gross weight of the UAV was 2730 g (Table 2). The sequential procedure of the release of water sampler and messenger during water capturing is shown in Figure 4. The sequential water capturing procedure is made of four events. At first, the FWCM is set by opening both end covers and fixing the messenger under the UAV to the servo lock. When the UAV is arrived at the sampling location, the FWCM is dropped into the water as the first event. The second event is the messenger release from the UAV after 4 s of dropping the FWCM. Once the messenger is released, it dives into water and hits the triggering mechanism on the FWCM. The third event is the water capturing by closing the side covers. The two side covers are closed due to the stretched rubber string inside the cartridge. Once the side covers are closed, water is trapped inside the cartridge. The rubber string keeps the two side covers tight and prevents potential leakage. The final event of the sequence is the UAV take off and return to home location. A delay time of 9 s is assigned before messenger release event and before take-off event. A video showing the system operation can be found in Koparan [40].

Table 2. Weights of the system components.

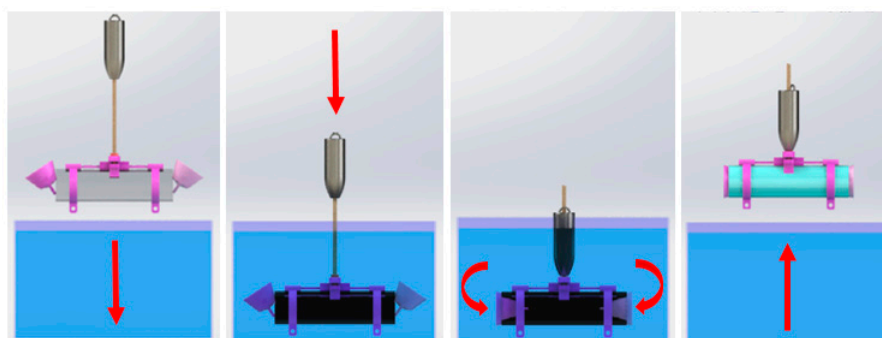| Component	Weight (g)
UAV	2333
Sampler	67
Messenger	200
Water sample	130
Gross weight	2730

Figure 4. Sequential procedure of water capturing with the FWCM mounted on the UAV.

2.4. Study Sites

The system was tested for its water sampling performance and autonomous flight quality over LaMaster Pond at Clemson University, Clemson SC. The latitude and longitude of LaMaster Pond are 34.6578544° N and −82.8193253° W, and the elevation of the pond is 216 m (709 ft) above the sea level according to the Clemson USGS quad topographic map [41]. The surface area of the pond was 1.1 ha. Because the UAV system did not have enough endurance capacity to travel every corner of the pond, three locations in the middle of the pond were selected for outdoor experiments as sampling locations. The center of the pond also allowed easy access by boat so traditional manual water sampling could be made to confirm the sampling results from the UAV-assisted water sampling system. The launch location for the autonomous missions is represented with the letter "0", and sampling locations are represented with numbers as shown in Figure 5. Water samples were collected within 2 m radius of the sampling points. The distances between launch location and sampling points 1, 2, and 3 were 52 m, 87 m, and 98 m, respectively. The coordinates of Sampling Point 1 were 34.657086° N and −82.819755° W, those of Sampling Point 2 were 34.656881° N and −82.819359° W, and those of Sampling Point 3 were 34.657187° N and −82.819279° W.
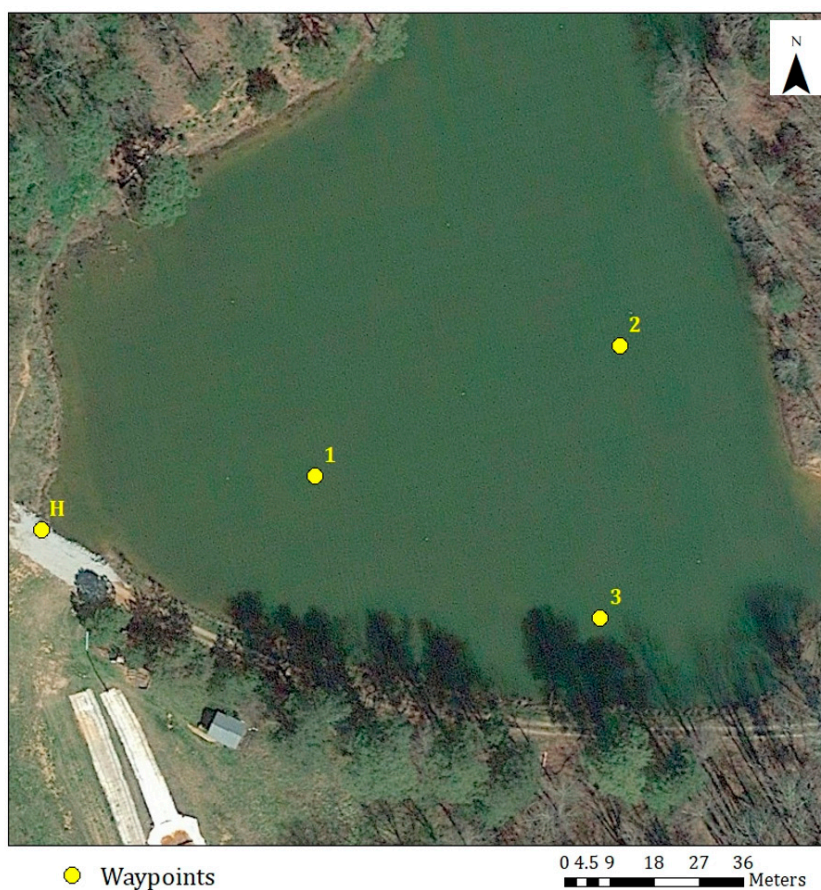
Figure 5. Water sampling waypoints on LaMaster Pond at Clemson University campus.

2.5. Manual Flights to Determine the UAV Water Sampler Performance

System components were initially tested indoors with the flight performance test station and adjustments were made until the desired flight performance was achieved. The FWCM was also tested to confirm the automatic activation function to be used during an autonomous water sampling mission in an outdoor environment. A 0.6 m^3 capacity water tank was used for the initial tests. The depth of water in the tank was 0.7 m. The surface area of the tank was 0.8 m^2. Each UAV-assisted sampling attempt was recorded based on their success. Individual water sampling attempts were made with individual manual flights. A total of 20 attempts were made to collect water samples using a radio controller. In order to determine the success rate of the sampler mechanism, the UAV was remotely operated using the "Loiter mode". Loiter mode allowed for relatively easy flight control over the water tank. The UAV was launched from a location with good GPS reception. The UAV was launched and controlled with the radio controller until the water sampler was inside the water tank. After the water sampler was dropped into the tank at a depth of approximately 0.4 m, the messenger was released by turning a designated switch on the radio controller. After releasing the messenger, the UAV ascended and returned to the launch location. The mission was recorded as a success if the water was captured by the sampler and the amount of water was measured. If the water sampler did not capture any water, the mission was recorded as a failure and the reasons for the failure were recorded.

2.6. Autonomous Flight Missions and Water Sampling Approach

The schematic diagram of a UAV-assisted water sampling operation is shown in Figure 6. Individual autonomous flight missions were conducted for each water collection flights. The sampling mechanism was set, the flight controller and power unit were connected, the motors were armed, and

the UAV was set to "idle mode" before each flight. In this mode, the UAV was ready to be launched by radio controller to start its mission. Next, "mission mode" was selected from the radio controller, and the flight controller searched for a preset mission. The throttle level was brought to 50% to provide enough thrust to start the mission. As soon as the motors started rotating at 50% throttle, the UAV ascended to the preset altitude and navigate to the predefined location. Once the UAV reached the sampling location, it descended to the sampling altitude and hovered for 18 s. During this time, the subsystem mounted on the UAV released the messenger weight to trigger the water sampler. After 18 s, water was captured and the UAV ascended to the navigation altitude to return to the launching location to complete the mission. An autonomous landing option was used to provide safe landing.
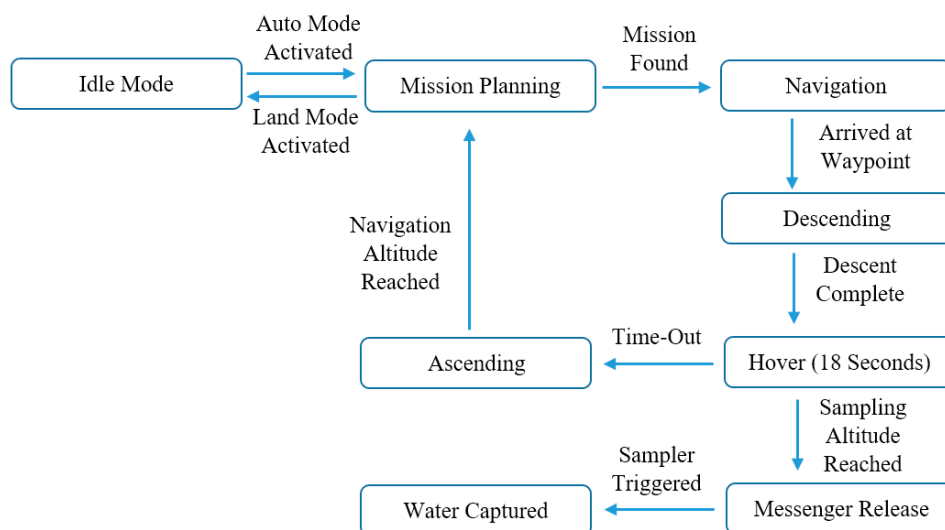

Figure 6. Schematic diagram showing the operation of the UAV-assisted water sampling.

Manual water samples were captured after each time the UAV ascended from the sampling point. A person in a kayak approached the same sampling point and captured the water sample at the same depth using an extendable wooden apparatus mounted water bottle. The time difference between the sample collections with two methods were less than 60 s. The extendible wooden apparatus was marked with measured lines to estimate the sampling depth. The water bottle was filled with approximately 300 mL of water sample but only 100 mL was used during measurements. Water samples were carried to the shore immediately after sampling for measurements. Both manual and UAV-assisted water samples were measured at the same time within 3 h on each sampling day.

Measured data was used to confirm that the UAV-assisted water sampling method can be replaced with the manual water sampling method. Water quality indices evaluated were dissolved oxygen (DO), temperature, electrical conductivity (EC), pH, and chloride. Temperature, pH, and DO measurements need to be made either in situ or on-site because these constituents cannot be analyzed adequately after transporting the sample to a laboratory [42]. Therefore, these parameters were measured on-site with handheld measurement sensors. Chloride ions were measured in the lab since these chemical properties do not change rapidly after sampling and filtering. In order to determine the consistency between manual and UAV-assisted water sampling, three replicates of water samples were collected at each sampling location and water quality constituent measurements were made.

2.7. Water Sampling Depth Estimation Procedure

Shallow samples are generally collected from surface waters at a depth of 0–25 cm or from the surface, and deep samples are taken from surface waters at a depth of more than 100 cm [43]. The water sampler was suspended from the UAV with a 1.8-m-long tether. Once the approximate altitude of the UAV was determined from the flight controller, sampling depth was estimated by calculating the

difference between the tether length and the altitude of the UAV during water sampling. The altitude data collection was made while flying the UAV autonomously during a water sampling mission (Figure 7).

The altitude data was retrieved from the flight controller using the MAVLink protocol [44]. The control tuning (CTUN) registrar is where the altitude information of autonomous flights are stored in the flight controller [45]. CTUN registrar information includes the barometer altitude (BarAlt), the desired altitude (DAlt), and the inertial navigation altitude estimate (Alt) that is driven from filtering algorithms [46]. The filtering algorithms are used to estimate the position, velocity and angular orientation based on gyroscope, accelerometer, compass, GPS, airspeed, and barometric pressure [47,48]. Therefore, the autonomous navigation and the altitude estimations of the UAV were dependent on all the sensor inputs and filtering algorithm. Because the altitude of the UAV was dependent on the listed sensors and filtering algorithms, their individual altitude outputs from the UAV were similar (Figure 8). Since an approximate altitude was needed for this study, only the barometer altitude outputs were used to estimate the sampling depth.
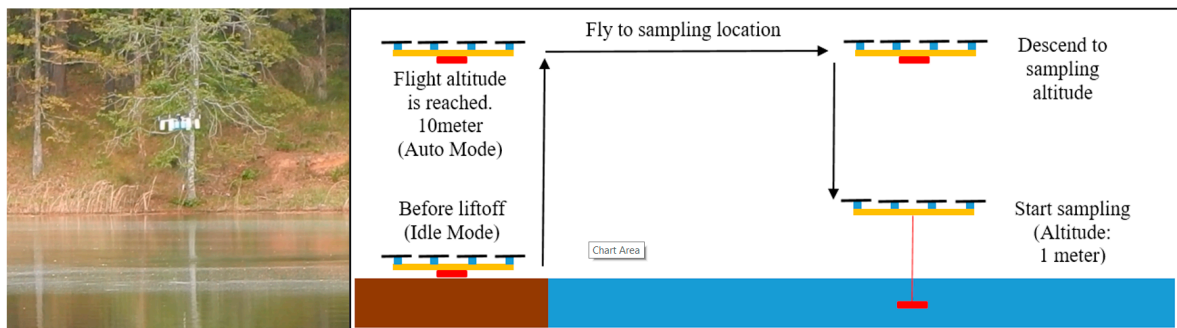

Figure 7. UAV with FWCM hovering at water sampling altitude during an autonomous flight (**left**) and autonomous flight path for aerial water sampling (**right**).

2.8. Water Quality Measurement Procedure

Water quality parameters including pH, DO, EC, temperature, and chloride were measured from both manual and UAV-assisted water samples. A Sension156 portable multi-meter (Hach, Loveland, CO, USA) was used to measure pH and EC. An HQ10 portable DO meter (Hach, Loveland, CO, USA) was used to measure DO and temperature. Chloride measurements were made using a DR/2400 spectrophotometer (Hach, Loveland, CO, USA). Each collected water sample was poured into a beaker for on-site measurements and results were recorded manually. Probes were rinsed with deionized water after each sampling and during calibration. A field notebook of water sampling and on-site analysis information sheet was used to record data. After on-site measurements, water samples were stored and transported to the lab for chloride measurements.

2.9. Data Analysis

Analysis on recorded CTUN altitude data was conducted to determine if the average altitude was 1.0 m above the water surface during 18 s of water sampling duration. The total autonomous flight time was 1.5 min for each mission and only 18 s of this time was used for hovering over water surface during sample collection (Figure 8). Figure 8 shows the relationship between barometric altitude estimation (BarAlt), desired altitude (DAlt), and inertial navigation altitude estimate (Alt) that was recorded during one of the autonomous water sampling mission.

When the UAV hovers at 1.0 m altitude from water surface, the water sampling depth would be taken as 0.8 m since the total length of the tether was 1.8 m. Barometric altitude data from three dependent runs were retrieved from Matlab® (R2017a, MathWorks, Natick, MA, USA) output. In each of the three dependent runs, there were 180 altitude measurements. These measurements

were dependent replicates. Data were recorded with 100 ms intervals [46]. In this case, these 180 barometer altitude data points represent the altitude measurements during the 18 s of hovering. Weather conditions during the autonomous flight experiments are shown in Table 3. Ambient weather condition information was retrieved from a commonly available smartphone application named "Weather" (Apple, Cupertino, CA, USA). The weather data was used to monitor overall weather conditions to decide whether to fly the UAV or not. If the weather forecast indicates rain, storm, or high wind speeds, then the conditions would not be suitable for flying the UAV.
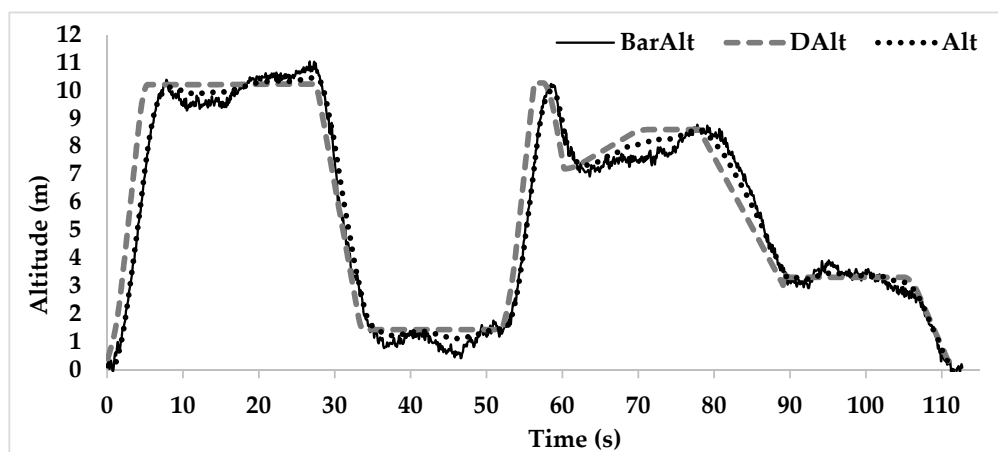

Figure 8. The altitude estimations of barometer (BarAlt), desired altitude (DAlt), and inertial navigation altitude estimate (Alt) are from one of the autonomous water sampling flight missions. The altitude estimations retrieved from the UAV while it was hovering during water sampling (18 s).

Table 3. Autonomous flight information for altitude range experiments.

Test No.	Data Log No.	Date	Time	Temperature (°C)	Wind Speed (km/h)	Humidity (%)
1	17-26-11	3 May 2016	4:47 pm	21.67	22.53	44
2	20-04-41	4 May 2016	5:11 pm	27.78	11.27	57
3	17-30-15	9 May 2016	5:33 pm	27.78	14.48	33

The collected water quality data were used to understand if the water quality measurements differ between two sampling methods: manual and UAV-assisted. In addition, an analysis was conducted to determine the actual water sampling depth during autonomous water sampling mission.

Water samples were collected in summer between 6 and 15 July 2016. The first four days of sampling (6–9 July) and the last five days of sampling (11–15 July) were made continuously. Because of weather conditions, water samples were not collected on 10 July. We hypothesized that the water quality constituent measurements were the same for the samples collected from the manual water sampling method and from the UAV-assisted water sampling method. For each water quality parameter, a mixed effects model was used to compare the UAV-assisted and manual methods of data collection. Day, method, and day–method interactions were the fixed effects, and location within day was included as a random effect.

3. Results and Discussion

The surface area of the pond was 1.1 ha. The total time for unpacking the system and setting up the ground station, launching missions for a total of 9 water samples at three different locations, on-site water quality measurements, and packing the system was approximately one hour. This time frame included UAV pre-flight checks, battery level check, motor and ESC cool down, and data retrieval from the flight controller for altitude estimation. In a normal water sampling trial, this time can

be reduced to less than 20 min because data retrieval will not be necessary and the motor and ESC cooldown will not be required. Total time for accessing the three different water sampling locations by kayak, obtaining water samples by hand, and analyzing them on-site was approximately 50 min. The sampling points were relatively close to each other, so traveling by kayak between sampling points did not take long, and the total time with manual sampling was shorter than UAV-assisted sampling.

3.1. Payload Capacity and Endurance

As external forces affect basic motions of the UAV, it was decided to measure the actual thrust that the UAV could produce with indoor laboratory tests. The change in thrust and endurance were recorded at throttle levels from 40 to 100%. Figure 9 shows the change in thrust over time while operating the UAV at 50% throttle. The averages of the thrust and endurance at each throttle level were calculated and used to develop the flight performance chart (Figure 10). Indoor flight performance test results showed that, when throttle level increased, the produced thrust also increased while endurance decreased. Total weight of the UAV with payload was 2730 g (Table 2). Therefore, the UAV must be able to produce enough thrust for liftoff with a minimum of 2730 g of weight. In addition to the total weight of the UAV, at 50% throttle, the UAV was able to produce an additional 10.3 N of thrust in lab conditions. These test results proved that the UAV could fly autonomously for 5.79 min when the throttle level for autonomous flight was set at 50%.
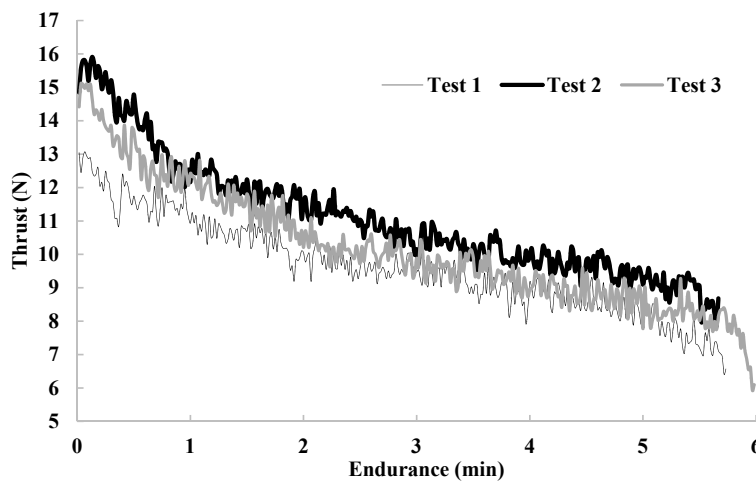

Figure 9. Change of thrust with endurance of the UAV at 50% throttle level.
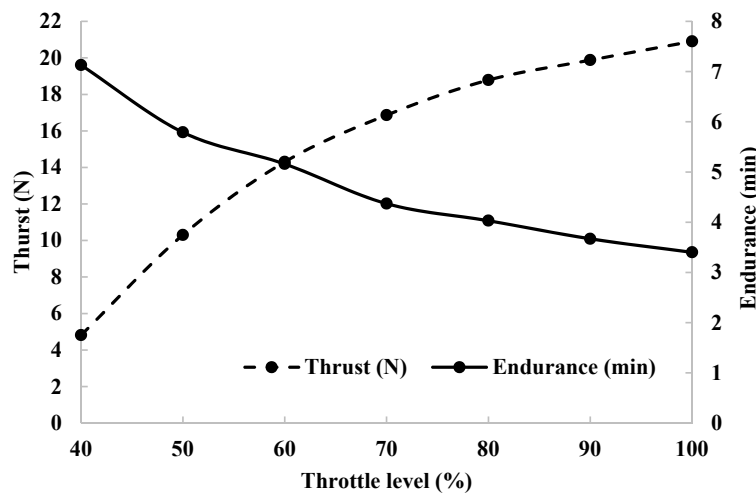

Figure 10. UAV indoor flight performance test results.

3.2. Estimation of Water Sampling Depth

Using a mixed-effects model procedure, the mean aircraft altitude was significantly different among the flights using a 0.05 level of significance (t (537) = 14.24, $p \leq 0.0001$). The mean water sampling altitude of the UAV for the first flight was 1.02 m with a standard deviation of 0.24, and for the third flight was 1.01 m with a standard deviation of 0.17. However, the mean water sampling altitude of the UAV for the second flight was 1.24 m with a standard deviation of 0.25 (Table 4).

Table 4. Descriptive statistics for water sampling altitude of the UAV.

Flight	No. of Measurements	Mean Altitude (m)	SD	Minimum (m)	Maximum (m)
First	180	1.02	0.24	0.56	1.61
Second	180	1.24	0.25	0.67	1.81
Third	180	1.01	0.17	0.67	1.72

Since the water sampler is suspended from the UAV with a 1.8 m tether, the water sampler was expected to be 0.56 m deep in the water while the UAV was hovering at 1.24 m altitude. On the other hand, the water sampler was expected to be 0.79 m deep in the water while UAV was hovering at 1.012 m altitude. The water sampling depth for this system ranged between 0.56 and 0.79 m based on barometer altitude estimates.

3.3. Experimental Results of Water Sampler Performance

3.3.1. Autonomous Flights for Water Sampling

Preliminary tests were conducted by operating the UAV with the radio controller in manual mode. For the preliminary tests, water samples were collected from an outdoor water tank. Water sampler was successfully activated remotely, and water was captured 12 times out of 20 manual sampling trials. The success rate of the automated water sampling was 60%. The reasons for the unsuccessful water collection attempts were due to operator errors and the tension on servo motor caused by the weight of the messenger. The operator errors were minimized with practice, and tension on the motor was minimized by redesigning the messenger attachment to the servo shaft. After correcting the functions of the water sampling mechanism, the system was ready for autonomous water collection missions.

A total of 73 autonomous water sampling flights were launched at LaMaster Pond. Preflight checks for autonomous water sampling missions were made before each flight. Total flight time, air temperature, wind speed, and humidity were recorded for each sampling day. Missions with collected water samples were recorded as successful missions and missions that did not collect water samples were recorded as unsuccessful missions. Among 73 flight missions, 48 of them were recorded as successful missions (66%) and 25 of them were recorded as unsuccessful missions (34%). Twenty of the unsuccessful water sampling missions were due to messenger malfunction and another 4 were due to servo motor malfunction. Upgrading the servo motor from a plastic gear to a metal gear would minimize the likelihood of servo malfunction. Only one of the missions were unsuccessful due to UAV stability. For this failed mission, wind speed was greater than 28.97 km/h. At this wind speed, the stability of the UAV was weak and it crashed during landing. There were no stability issues recorded at wind speeds less than 24.14 km/h.

3.3.2. Comparison of UAV-Assisted and Manual Water Quality Data

Table 5 shows the summary statistics for quality parameters measured in water samples collected with UAV-assisted method and traditional manual water collection method. Average DO from UAV-assisted method was higher than the average DO measured from the manual method. There was a significant difference in the average DO between the manual method and UAV-assisted method (t (18) = −10.07, $p < 0.001$). Average pH measured from UAV-assisted method was higher than

the average pH measured from the manual method (t (18) = -3.28, p = 0.0042). Average chloride values were also significantly different between the two methods; average chloride measured from UAV-assisted method was higher than the average chloride measured from the manual method (t (18) = -12.08, $p < 0.001$). Chloride values were expected to be between 10 and 100 mg/L [49]. Therefore, the observed chloride variation in the pond was within the expected range. Although the difference between the two methods for chloride were statistically significant, the average difference between the two measurements was only 1.49 mg/L. This difference for chloride measurements could be due to typical sampling variations. Therefore, one can argue that the observed chloride variation was minimal. There was not a significant difference in the average EC values between the manual method and the UAV-assisted method (t (18) = -1.59, p = 0.129). There was no significant difference in average temperature between the manual method and UAV-assisted method (t (18) = -0.12, p = 0.909).

Table 5. Descriptive statistics for water quality parameters obtained by the two different methods.

Quality Parameter	UAV Method		Manual Method		Difference (%)	t Value (DF)	p Value
	Mean	SD	Mean	SD			
DO (mg/L)	7.18	0.02	6.93	0.02	3.6	-10.07 (18)	<0.001
EC (µS/cm)	76.04	0.76	74.32	0.76	2.3	-1.59 (18)	0.129
pH	5.34	0.03	5.30	0.03	0.76	-3.28 (18)	0.004
Temp. (°C)	30.12	0.09	30.11	0.09	0.03	-0.12 (18)	0.909
Chloride (mg/L)	5.46	0.08	3.97	0.08	37.5	-12.08 (18)	<0.001

Change in temperature was observed in water samples between the moments at which the water samples were poured into a beaker and the last measurement was made. The temperature change in the sample was observed as between 4 and 7 °C. Manual water sampling depth was adjusted by the person who made the manual sampling on a kayak. These adjustments were made based on the water sampling altitude of the UAV and were different at each sampling time. Although DO, pH, and chloride measurements were statistically different, the difference in measurements between the manual and UAV-assisted methods for collection for DO and pH were quite small. The percent differences calculated by comparing the mean quality parameters of UAV-assisted and manual methods. The percent difference values of measurements between two sampling methods show minimal error. The percent difference of DO and EC measurements between the two methods were only 3.6% and 2.3%. For pH and temperature, the percent differences were less than 1%. The difference between the mean chlorides measured for the methods was 1.49 mg/L.

4. Conclusions

An autonomous water sampling system containing a UAV and water capturing mechanism was developed and tested with indoor and outdoor experiments. The system performed autonomous water sampling tasks by collecting water samples with an average of 130 mL at 0.56–0.79 m depths. The system autonomously collected water samples at wind speeds less than 24.14 km/h. The UAV caused minimal turbulence on water surfaces while hovering compared to windy conditions with wind speeds greater than 24.14 km/h (15 mph). The system was tested for its consistency regarding water constituent measurements. Measured average EC and temperature values were not statistically different between the manual and UAV-assisted sampling methods. DO and pH measurements were statistically different with differences of 3.6% and 2.3%, respectively. These differences for DO and pH measurements were a function of error range of the measuring instruments ($\pm$0.2 mg/L for DO meter and $\pm$0.01 for pH meter). The difference between the two methods for chloride measurements was 37.5%. The differences for the measured DO, pH, and chloride between the methods might be due to the temperature difference in water samples. Therefore, a different approach for determining the consistency between two methods would provide more accurate results.

The UAV-assisted water sampling had little impact on the time required for water sampling because of the size of the pond used for this study. The set-up process for the UAV-assisted water sampling, safety and pre-flight checks, and battery replacement between the flight missions took most of the time. The system would be more useful if it were used for sampling from larger waterbodies with greater surface areas. For each water sampling, a single battery was used. The highest amount of battery capacity was consumed for the longest sampling point mission (98 m). The UAV used for this study can navigate up to 196 m with a single battery, collect water samples, and safely return to the home location. The distance that the UAV travels would be longer if a battery with higher capacity is used.

In addition, a UAV-assisted water sampling system could provide advantages in water sampling sites that are not easy to access. A waterbody that presents access difficulties may be ideal to test whether the UAV-assisted water sampling system can reduce overall sampling time. The system can land on water surfaces and obtain water samples while floating on the water. The landing option during water sampling might provide advantages during water sampling in fast-flowing water, but further experiments are necessary. The UAV-assisted water sampler can certainly be used by field operators and scientists for remote water sampling to improve the resolution of water quality data.

References

1. Thomas, K.V.; Hurst, M.R.; Matthiessen, P.; Sheahan, D.; Williams, R.J. Toxicity characterisation of organic contaminants in stormwaters from an agricultural headwater stream in south east England. *Water Res.* **2001**, *35*, 2411–2416. [CrossRef]
2. Liu, R.; Xu, F.; Zhang, P.; Yu, W.; Men, C. Identifying non-point source critical source areas based on multi-factors at a basin scale with swat. *J. Hydrol.* **2016**, *533*, 379–388. [CrossRef]
3. Ma, Y.; Egodawatta, P.; McGree, J.; Liu, A.; Goonetilleke, A. Human health risk assessment of heavy metals in urban stormwater. *Sci. Total Environ.* **2016**, *557–558*, 764–772. [CrossRef] [PubMed]
4. Neumann, M.; Liess, M.; Schulz, R. A qualitative sampling method for monitoring water quality in temporary channels or point sources and its application to pesticide contamination. *Chemosphere* **2003**, *51*, 509–513. [CrossRef]
5. Van der Merwe, D. Cyanobacterial (Blue-Green Algae) Toxins. In *Handbook of Toxicology of Chemical Warfare Agents*, 2nd ed.; Gupta, R.C., Ed.; Academic Press: Boston, MA, USA, 2015; Chapter 31; pp. 421–429.
6. McGowan, S.; Sivanpillai, J.F.; Ramesh, S. *Algal Blooms in Biological and Environmental Hazards, Risks, and Disasters, 5–43*; Boston Academic Press: Boston, MA, USA, 2016.
7. Peters, C.B.; Zhan, Y.; Schwartz, M.W.; Godoy, L.; Ballard, H.L. Trusting land to volunteers: How and why land trusts involve volunteers in ecological monitoring. *Biol. Conserv.* **2016**, *208*, 48–54. [CrossRef]
8. EPA. Volunteer Stream Monitoring: A Methods Manual. EPA 841-b-97-003. 1997. Available online: https://www.Epa.Gov/sites/production/files/2015-06/documents/stream.pdf (accessed on 10 March 2017).
9. Mesner, N.; Geiger, J. Understanding Your Watershed: Ph. Utah State University. Water Quality Extension. 2010. Available online: http://extension.Usu.Edu/files/publications/publication/nr_wq_2005-19.pdf (accessed on 3 February 2017).
10. Chung, W.Y.; Yoo, J.H. Remote water quality monitoring in wide area. *Sens. Actuators B Chem.* **2015**, *217*, 51–57. [CrossRef]

11. Park, D.M.; McCarty, L.B.; White, S.A. *Interpreting Irrigation Water Quality Reports*; Clemson University Water Chemistry: Clemson, SC, USA, 2016.

12. Schulte, E.E.; Soil and Applied Chlorine. Understanding Plant Nutrients. 1999. Available online: Http://corn.Agronomy.Wisc.Edu/management/pdfs/a3556.Pdf (accessed on 26 April 2016).

13. Kaizu, Y.; Iio, M.; Yamada, H.; Noguchi, N. Development of unmanned airboat for water-quality mapping. *Biosyst. Eng.* **2011**, *109*, 338–347. [CrossRef]

14. Karimanzira, D.; Jacobi, M.; Pfuetzenreuter, T.; Rauschenbach, T.; Eichhorn, M.; Taubert, R.; Ament, C. First testing of an AUV mission planning and guidance system for water quality monitoring and fish behavior observation in net cage fish farming. *Inf. Proc. Agric.* **2014**, *1*, 131–140. [CrossRef]

15. Freeman, P.K.; Freeland, R.S. Agricultural UAVs in the U.S.: Potential, policy, and hype. *Remote Sens. Appl. Soc. Environ.* **2015**, *2*, 35–43. [CrossRef]

16. Schut, A.G.T.; Traore, P.C.S.; Blaes, X.; de By, R.A. Assessing yield and fertilizer response in heterogeneous smallholder fields with UAVs and satellites. *Field Crops Res.* **2018**, *221*, 98–107. [CrossRef]

17. Chang, A.; Jung, J.; Maeda, M.M.; Landivar, J. Crop height monitoring with digital imagery from unmanned aerial system (UAS). *Comput. Electron. Agric.* **2017**, *141*, 232–237. [CrossRef]

18. Pérez-Ortiz, M.; Peña, J.M.; Gutiérrez, P.A.; Torres-Sánchez, J.; Hervás-Martínez, C.; López-Granados, F. Selecting patterns and features for between- and within- crop-row weed mapping using UAV-imagery. *Expert Syst. Appl.* **2016**, *47*, 85–94. [CrossRef]

19. Bendig, J.; Yu, K.; Aasen, H.; Bolten, A.; Bennertz, S.; Broscheit, J.; Gnyp, M.L.; Bareth, G. Combining UAV-based plant height from crop surface models, visible, and near infrared vegetation indices for biomass monitoring in barley. *Int. J. Appl. Earth Obs. Geoinf.* **2015**, *39*, 79–87. [CrossRef]

20. Villa, T.; Gonzalez, F.; Miljievic, B.; Ristovski, Z.; Morawska, L. An overview of small unmanned aerial vehicles for air quality measurements: Present applications and future prospectives. *Sensors* **2016**, *16*, 1072. [CrossRef] [PubMed]

21. Snaddon, J.; Petrokofsky, G.; Jepson, P.; Willis, K.J. Biodiversity technologies: Tools as change agents. *Biol. Lett.* **2013**, *9*, 20121029. [CrossRef] [PubMed]

22. Koc, C. Design and Development of a Low-Cost UAV for Pesticide Applications. *JAFAG* **2017**, *34*, 94–103. [CrossRef]

23. Gallacher, D. Drone applications for environmental management in urban spaces: A review. *Int. J. Sustain. Land Use Urban Plan.* **2017**, *3*, 1–14. [CrossRef]

24. Rutkin, A. Blood delivered by drone. *New Sci.* **2016**, *232*, 24. [CrossRef]

25. Van de Voorde, P.; Gautama, S.; Momont, A.; Ionescu, C.M.; De Paepe, P.; Fraeyman, N. The drone ambulance [a-uas]: Golden bullet or just a blank? *Resuscitation* **2017**, *116*, 46–48. [CrossRef] [PubMed]

26. Rabta, B.; Wankmüller, C.; Reiner, G. A drone fleet model for last-mile distribution in disaster relief operations. *Int. J. Disaster Risk Reduct.* **2018**, *28*, 107–112. [CrossRef]

27. Rusnák, M.; Sládek, J.; Kidová, A.; Lehotský, M. Template for high-resolution river landscape mapping using uav technology. *Measurement* **2018**, *115*, 139–151. [CrossRef]

28. Zeng, C.; Richardson, M.; King, D.J. The impacts of environmental variables on water reflectance measured using a lightweight unmanned aerial vehicle (UAV)-based spectrometer system. *ISPRS J. Photogramm. Remote Sens.* **2017**, *130*, 217–230. [CrossRef]

29. Cook, K.L. An evaluation of the effectiveness of low-cost UAVs and structure from motion for geomorphic change detection. *Geomorphology* **2017**, *278*, 195–208. [CrossRef]

30. Koparan, C.; Koc, A.; Privette, C.; Sawyer, C. In situ water quality measurements using an unmanned aerial vehicle (UAV) system. *Water* **2018**, *10*, 264. [CrossRef]

31. Ore, J.-P.; Elbaum, S.; Burgin, A.; Zhao, B.; Detweiler, C. Autonomous aerial water sampling. In *Field and Service Robotics: Results of the 9th International Conference*; Mejias, L., Corke, P., Roberts, J., Eds.; Springer: Cham, Switzerland, 2015; pp. 137–151.

32. Gupta, A.K.; Jha, V. Design and development of remote controlled autonomous synchronic hexaroter aerial (ASHA) robot. *Procedia Technol.* **2014**, *14*, 51–58. [CrossRef]

33. Karki, J. Signal Conditioning Wheatstone Resistive Bridge Sensors. Texas Instruments, Application Report. SLOA034. 1999. Available online: http://www.ti.com/lit/an/sloa034/sloa034.pdf (accessed on 12 March 2017).

34. Panagiotou, P.; Tsavlidis, I.; Yakinthos, K. Conceptual design of a hybrid solar male UAV. *Aerosp. Sci. Technol.* **2016**, *53*, 207–219. [CrossRef]

35. Wilde, F.D. Preparations for water sampling. In *National Field Manual for the Collection of Water-Quality Data U.S. Geological Survey Techniques of Water-Resources Investigations, Book 9*; U.S. Geological Survey: Reston, VA, USA, 2005.

36. NIST. *National Institute of Standards and Technologies: Field Sampling Procedures for Fuel and Motor Oil Quality Testing*; Nist Handbook; U.S. Department of Commerce: Washington, DC, USA, 2016; p. 12.

37. Gade, M.M.; Hangal, S.; Krishnan, D.; Arya, H. Development of obstacle avoidance controller for MAVs: Testing in hardware-in-loop simulation. In Proceedings of the 4th IFAC Conference on Advances in Control and Optimization of Dynamical Systems ACODS 2016, Tiruchirappalli, India, 1–5 February 2016; Volume 49, pp. 413–418.

38. Polo, J.; Hornero, G.; Duijneveld, C.; García, A.; Casas, O. Design of a low-cost wireless sensor network with uav mobile node for agricultural applications. *Comput. Electron. Agric.* **2015**, *119*, 19–32. [CrossRef]

39. Chao, H.; Luo, Y.; Di, L.; Chen, Y.Q. Roll-channel fractional order controller design for a small fixed-wing unmanned aerial vehicle. *Control Eng. Pract. Spec. Issue Aer. Robot.* **2010**, *18*, 761–772. [CrossRef]

40. Koparan, C. UAV-Assisted Autonomous Water Sampling [Video File]. 2016. Available online: https://www.youtube.com/watch?V=zugmxe_jppm (accessed on 2 April 2018).

41. LamasterPondTopo. Lamaster Pond Topo Map in Pickens County Sc. 2016. Available online: http://www.Topozone.Com/south-carolina/pickens-sc/reservoir/lamaster-pond/ (accessed on 15 July 2016).

42. Paschke, A. Consideration of the physicochemical properties of sample matrices—An important step in sampling and sample preparation. *TRAC Trends Anal. Chem.* **2003**, *22*, 78–89. [CrossRef]

43. Wang, X. Reprint of "China geochemical baselines: Sampling methodology". *Cont. Reg. Local Scale Geochem. Mapp.* **2015**, *154*, 17–31. [CrossRef]

44. MAVLink. Mavlink Micro Air Vehicle Communication Protocol. 2016. Available online: http://qgroundcontrol.Org/mavlink/start (accessed on 18 July 2016).

45. Salvador, B.; Moreno, J.C.; Guzman, J.L. Modelling of a non-commercial UAV for control and robotics laboratory. *IFAC-PapersOnLine* **2015**, *48*, 65–69. [CrossRef]

46. ArduPilot. Downloading and Analyzing Data Logs in Mission Planner. 2016. Available online: http://ardupilot.Org/copter/docs/common-downloading-and-analyzing-data-logs-in-mission-planner.html (accessed on 10 July 2016).

47. Ardupilot. Ekf2 Estimation System. 2016. Available online: http://ardupilot.Org/dev/docs/ekf2-estimation-system.html (accessed on 27 April 2018).

48. Gitbooks. Altitude Hold. 2016. Available online: https://erlerobotics.Gitbooks.Io/erle-robotics-mav-tools-free/content/en/understanding_a_log_file/altitude_hold.html. (accessed on 27 April 2018).

49. Ore, J.P.; Elbaum, S.; Burgin, A.; Detweiler, C. Autonomous aerial water sampling. *J. Field Robot.* **2015**, *32*, 1095–1113. [CrossRef]